



Functionalized Acyclic (L)-Threoninol Nucleic Acid Four-Way Junction with High Stability In Vitro and In Vivo

Anders Märcher[†], Vipin Kumar[†], Veronica L. Andersen, Kassem El-Chami, Thuy J. D. Nguyen, Mads K. Skaanning, Imke Rudnik-Jansen, Jesper S. Nielsen, Kenneth A. Howard, Jørgen Kjems, and Kurt V. Gothelf*

Abstract: Oligonucleotides are increasingly being used as a programmable connection material to assemble molecules and proteins in well-defined structures. For the application of such assemblies for in vivo diagnostics or therapeutics it is crucial that the oligonucleotides form highly stable, non-toxic, and non-immunogenic structures. Only few oligonucleotide derivatives fulfil all of these requirements. Here we report on the application of acyclic L-threoninol nucleic acid (aTNA) to form a four-way junction (4WJ) that is highly stable and enables facile assembly of components for in vivo treatment and imaging. The aTNA 4WJ is serum-stable, shows no non-targeted uptake or cytotoxicity, and invokes no innate immune response. As a proof of concept, we modify the 4WJ with a cancer-targeting and a serum half-life extension moiety and show the effect of these functionalized 4WJs in vitro and in vivo, respectively.

In recent years oligonucleotide junctions have increasingly been used as a tool to assemble biomolecules into multifunctional structures. Branched DNA structures such as mobile 4-way junctions (4WJ) also known as Holiday junctions are found in nature. Seeman and co-workers were the first to make artificial immobile four-way junctions (4WJs) and most of the DNA structures that have been designed are based on 4WJs as the fundamental motif.^[1] In 2014 Gartner and co-workers reported on the assembly of DNA–protein conjugates in various junction structures.^[2] In 2020 Pan et al. used a DNA 4WJ of mirror image DNA ((L)-DNA) to combine different antigen recognizing proteins, thereby, increasing T cell engaging and in vivo tumour killing.^[3] Multiple other DNA structures than 4WJs have also been

utilized for biomolecular assembly e.g. in 2016, Jiang and co-workers used a DNA tetrahedron for single-photon emission computed tomography (SPECT).^[4] A commonly used setup with different DNA nanostructures, is the targeted delivery of the DNA intercalator doxorubicin, which has been shown for diverse DNA constructs.^[5–7]

A disadvantage of the DNA structures is that DNA is *de facto* a biodegradable polymer which severely hampers the in vivo half-life and general serum stability. Two other issues are that relatively large junctions are required when only using DNA, because of the limited thermal stability and that DNA oligos can potentially activate the immune system.^[8] A possible solution to address the stability issues, is the use of artificial or modified oligonucleotides. Two important classes of artificial and modified oligonucleotides are peptide nucleic acid (PNA) and locked nucleic acid (LNA) respectively. They can both form highly stable hetero-duplex structures with DNA and homo-duplexes with themselves.^[9,10]

The first preparation of a 4WJ using artificial oligonucleotides is to our knowledge from 2008, here a glycerol nucleic acid (GNA) junction is prepared. Only the stability and folding of the junction was investigated.^[11] In 2013 Kazane et al. reported on the design of PNA dimers and 4WJs which were used to assemble recombinant FABs in homo- and heteromeric assemblies.^[12] The structures were tested in vitro and showed higher efficiency than bispecific antibodies. Later, in 2019 Andersen and co-workers developed a 4WJ scaffold with only 6 basepair (bp) arms using a combination of 2'-OMe and LNA nucleotides. They did multiple studies to prove the junction's in vivo capabilities, and prepared constructs that were used for targeting and imaging of the liver.^[13] However the chemical synthesis required to prepare LNA is very challenging and requires a minimum of 15 chemical steps to reach just one of the four

[*] Dr. A. Märcher, Dr. V. Kumar, K. El-Chami, Dr. T. J. D. Nguyen, M. K. Skaanning, Prof. Dr. K. V. Gothelf
 Department of Chemistry and Interdisciplinary Nanoscience Centre (iNANO), Aarhus University
 Gustav Wieds Vej 14, 8000 Aarhus (Denmark)
 E-mail: kvg@chem.au.dk

Dr. V. L. Andersen, Dr. J. S. Nielsen, Prof. Dr. J. Kjems
 Department of Molecular Biology and Genetics, and Interdisciplinary Nanoscience Centre (iNANO),
 Aarhus University
 Gustav Wieds Vej 14, 8000 Aarhus (Denmark)

Dr. I. Rudnik-Jansen, Prof. Dr. K. A. Howard
 Interdisciplinary Nanoscience Centre (iNANO),
 Aarhus University
 Gustav Wieds Vej 14, 8000 Aarhus (Denmark)

[†] These authors contributed equally to this work.

© 2022 The Authors. Angewandte Chemie International Edition published by Wiley-VCH GmbH. This is an open access article under the terms of the Creative Commons Attribution Non-Commercial NoDerivs License, which permits use and distribution in any medium, provided the original work is properly cited, the use is non-commercial and no modifications or adaptations are made.

required phosphoramidites.^[14,15] In PNA the normal phosphate backbone is replaced with a neutral peptide backbone. This allows PNA to form a duplex with DNA under lower salt concentrations than normally required, but it also means that PNA suffers from solubility issues in aqueous buffer.^[16]

Other more readily available nucleotide analogues such as 2'-MeO, 2'-F derivatives, thiophosphates and (L)-DNA that are relatively resistant to degradation by nucleases may potentially also be used to form such junctions. These are easier to prepare, and therefore more readily available, however, contrary to LNA and PNA that form very stable duplexes, the thermal stability of duplexes of 2'-MeO, 2'-F derivatives, thiophosphates, and also (L)-DNA have similar stability as DNA (see above) and thus larger structures are therefore needed, which in term increases the cost and complexity.

In this study we investigate the lesser-known acyclic L-threoninol nucleic acids (aTNA) for its applicability to form a 4WJ that can be used in vivo. Asanuma et al. were the first to report on the synthesis of aTNA and that aTNA forms an antiparallel homo-duplex of high stability.^[17,18] We have later shown that aTNA forms highly stable sandwich type triplex structures with DNA and RNA and that aTNA is capable of forming i-motifs and G-quadruplexes.^[19–22] This artificial oligonucleotide furthermore forms parallel duplexes with DNA and RNA, presumably because of an optimal rigidity.^[17] While aTNA has some structural similarities with PNA with respect to the acetamide linker between the backbone and the bases, the phosphate backbone is conserved in aTNA and therefore it is highly soluble in water.

Herein, we report the synthesis of four unique aTNA strands that form a four-way junction (4WJ) in quantitative yield, when the four strands are mixed in equimolar amounts. The concept is outlined in Figure 1. We envisioned that each strand could be modified with 5' amino groups to allow functionalization of each strand to address different in vivo needs. Thus, up to four functionalities for e.g. targeting, imaging, or drug delivery can easily be combined without the need for elaborate bioconjugation. Different non-natural oligonucleotide 4WJs have been prepared previously, but to our knowledge only one system has been developed with in vivo use, and in this case LNA is utilized.^[13]

We propose that aTNA may be an ideal material to form a 4WJ for in vivo use as it forms highly stable homo-duplexes, and the chemical synthesis is much less demanding than for LNA. In our lab each aTNA phosphoramidite (guanine, cytosine, adenine, thymine) is currently being prepared in a decagram scale in 5 to 10 chemical steps in a convergent synthesis. Especially the relative few chemical steps, compared to LNA, makes it much more convenient to produce large scale aTNA oligos compared to preparing LNA oligos.

Four unique aTNA strands (aTNA-A, aTNA-B, aTNA-C and aTNA-D) with sixteen aTNA nucleotides in each strand were prepared for the aTNA 4WJ. The sequence for each strand was chosen based on a previous design of an immobile DNA 4WJ by Kallenbach and co-workers.^[1] The

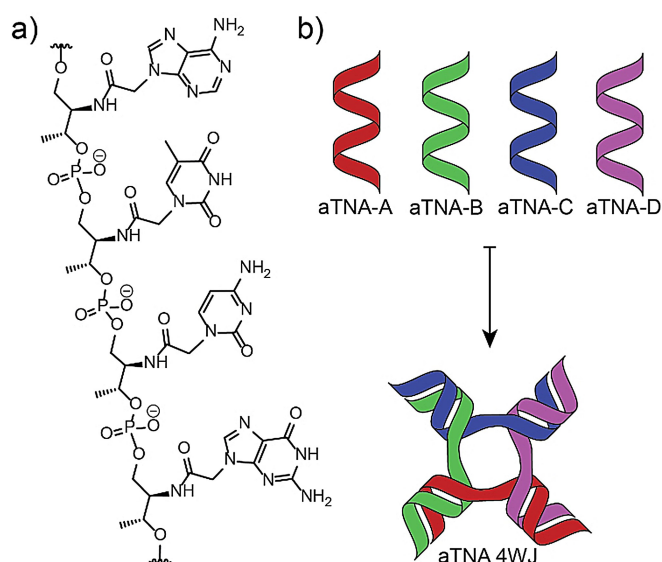


Figure 1. a) Structure of a section of an aTNA oligo with each base (cytosine, thymine, guanine and adenine) shown. b) Illustration of the principle of the aTNA 4WJ junction. Four unique strands, aTNA-A, aTNA-B, aTNA-C and aTNA-D assemble into aTNA 4WJ when incubated together.

4WJ contains eight aTNA base pairs in each of the four arms. We first attempted to investigate the formation of the 4WJ using native gel electrophoresis, but since it is difficult to visualize aTNA using traditional nucleotide staining, an amino modified aTNA-C was functionalized with Cyanine5 (Cy5). The amino-modified strand was reacted with a Cy5-NHS ester using standard DNA chemistry. After purification, this yielded the Cy5 functionalized aTNA-C-Cy5 strand in excellent yield (Supporting Information Table S2), which was used for gel experiments in the rest of the study. When the four strands are mixed in equimolar ratio in PBS buffer for 30 min they fold into a single structure (Figure 2a). This structure, which is presumably the Cy5-4WJ, is only formed when all four strands are present. To verify that the

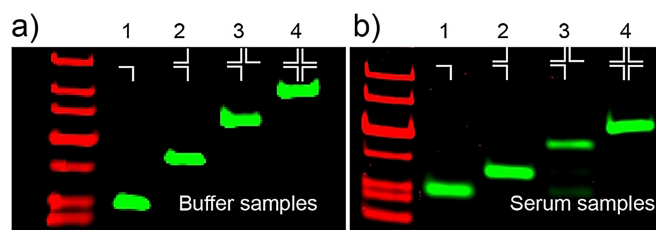


Figure 2. Formation and serum stability of the aTNA 4WJ analyzed by 4–20% native TBE gel electrophoresis. Each lane contains the same amount and type of aTNA. The amount is in all cases equimolar. Lane 1: aTNA-C-Cy5, Lane 2: Same as lane 1 + aTNA-D, Lane 3: Same as lane 2 + aTNA-A, Lane 4: Same as lane 3 + aTNA-B. a) Formation of the aTNA 4WJ. Oligos were incubated in PBS ON and then analyzed. b) Serum stability of the aTNA 4WJ, samples were incubated in PBS (50% FBS) at 37 °C for 24 h and then analyzed. Red is SybrGold scan, green is Cy5 scan. For full image see Figure S2 and Figure S3 in the Supporting Information.

observed bands in lane 4 is the 4WJ, the band was cut out of the gel and the content was analysed by LC-MS. Indeed, all four unique aTNA oligoes could be identified. To proof the modularity of the design approach we also prepared an aTNA 5WJ (Supporting Information Figure S7). Circular dichroism (CD) was recorded for single, two, three, and four aTNA strands to ensure that only one secondary structure was formed (Supporting Information Figure S1). For two strands and more a negative Cotton effect around 282 nm and a positive effect around 259 nm was observed which is characteristic for an aTNA duplex.^[19] These data indicate that, as expected, the only secondary structure found is an aTNA duplex.

We then investigated the thermal stability of the aTNA 4WJ compared to other DNA and aTNA complexes. All constructs were prepared with the same sequence and investigated in Dulbecco's PBS to allow for direct comparisons, the results are seen in Table 1. Thermal denaturing showed that a 16 bp aTNA homoduplex has a T_m of 86 °C which is significantly more stable than a similar DNA homoduplex with a T_m of 62 °C. The aTNA-DNA heteroduplex has a slightly lower T_m than the DNA homoduplex. The difference in homoduplex stability is even more pronounced for the aTNA and DNA 4WJ, with 8 bp in each arm. The DNA 4WJ melts at 31 °C which is 38 °C lower than the aTNA junction that melts at 69 °C. Furthermore 31 °C is below human body temperature of 37 °C, and the DNA 4WJ would therefore melt under these conditions. The aTNA 4WJ melts at a temperature that is slightly lower than the GNA 4WJ mentioned above, which is reported to melt at 76 °C.^[11] The GNA structure was prepared using almost the same sequence, however it has one DNA base-pair added at the end of each junction, which can possibly contribute to a slightly higher T_m .

The high thermal stability of the aTNA 4WJ makes it suitable for in vivo applications and hence we wanted to investigate its biocompatibility. Drug delivery and imaging constructs should show low cytotoxicity, innate immune response, and non-targeted uptake, to keep side effects to a minimum. Furthermore, it is highly important that such a construct is not rapidly degraded in serum.

The serum stability of the aTNA 4WJ was first tested. The junction was added to fetal bovine serum (FBS) at a final concentration of 50 % FBS and incubated for 24 h at 37 °C. Hereafter native gel analysis was performed, which showed no degradation of the aTNA-4WJ. (Figure 2b). This confirmed that the 4WJ is not a target for serum nucleases and that the 4WJ is compatible with salt concentrations found in serum.

Next, flow cytometry was used to test non-targeted uptake on KB cells which is a cancer cell line. The KB cells were treated with an aTNA single strand, an aTNA duplex, or the 4WJ. To allow for quantification of uptake an aTNA Cy5 strand was used for all constructs. The cells were analyzed after four hours with flow cytometry which showed no uptake for any of the constructs (Figure 3a). This may be an advantage for later specific targeting.

Cytotoxicity was investigated using human umbilical vein endothelial cells (HUVEC cells), these cells are frequently used as model system for normal endothelial cells.^[23] Different concentrations of aTNA, either single strand, duplex, or 4WJ were added to HUVEC cells for 24 h. Hereafter, the amount of live cells were quantified and compared to a PBS control (Figure 3b). No cytotoxicity was observed for any of the constructs investigated even at the highest concentration tested (200 $\mu\text{g mL}^{-1}$).

Finally, innate immune response of the aTNA 4WJ was assayed using human peripheral blood mononuclear cells

Table 1: Melting temperature for different aTNA and DNA complexes. Melting curves are found in the Supporting Information Figure S9–S13.

Entry	Oligo Name	Oligonucleotide Sequence ^[a]	Melting Temp. [°C]
aTNA duplex	aTNA-D	GCCATAGTGGATTGCGT	86
	aTNA-DC	CGCAATCCACTATGGCT	
DNA duplex	DNA-D	GCCATAGTGGATTGCGT	62
	DNA-DC1	CGCAATCCACTATGGC	
DNA-aTNA duplex	aTNA-D	GCCATAGTGGATTGCGT	57
	DNA-DC2	CGGTATCACCTAACGC	
DNA 4WJ	DNA-A	CGCAATCCTGAGCACGT	31 ^[11]
	DNA-B	CGTGCTCACCGAATGCT	
	DNA-C	GCATTGGACTATGGCT	
	DNA-D	GCCATAGTGGATTGCGT	
aTNA 4WJ	aTNA-A	CGCAATCCTGAGCACGT	69
	aTNA-B	CGTGCTCACCGAATGCT	
	aTNA-C	GCATTGGACTATGGCT	
	aTNA-D	GCCATAGTGGATTGCGT	

[a] Bold text indicates (L)-aTNA nucleotide. Melting temperature was investigated in Dulbecco's PBS.

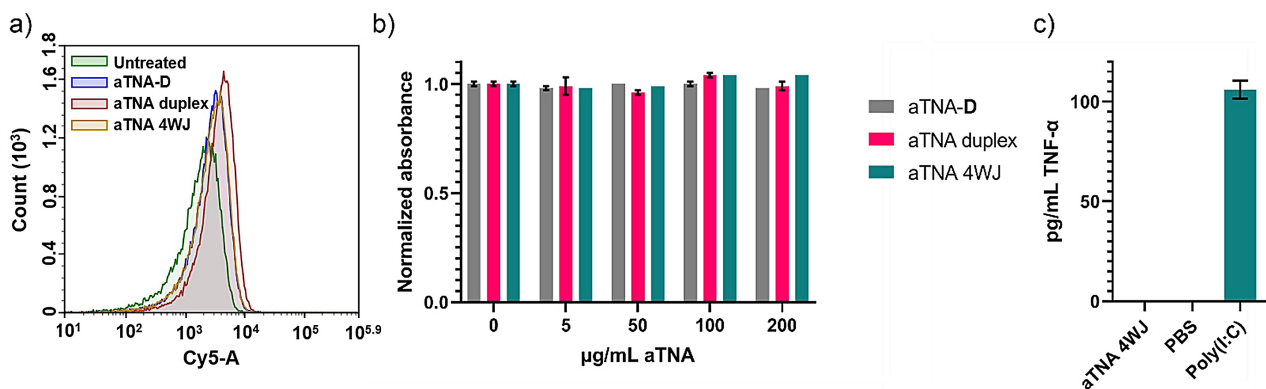


Figure 3. a) Non-targeted uptake of different aTNA constructs in KB cells investigated with flow cytometry. Cells were treated with Cy5 labeled aTNA structures or single strand being either aTNA-D, aTNA duplex (aTNA-D and aTNA-DC) or the aTNA 4WJ for 4 h in cell media with 5 % PBS. Samples were then washed thrice with PBS and analyzed with flow cytometry. b) Cytotoxicity of different aTNA constructs on HUVEC cells. Cells were treated with aTNA-D, aTNA duplex (aTNA-D and aTNA-DC) or the aTNA 4WJ in different concentrations in cell media with 5 % PBS. The cells were then grown overnight and amount of cells alive was quantified. c) Immunogenicity of the aTNA 4WJ investigated on PBMC. Cells were treated with either aTNA 4WJ, Poly(I:C) as a positive control, or PBS in cell media with 5 % PBS and left overnight. Cell supernatant was then collected and amount of TNF- α was quantified.

(PBMC). The cells were treated with either aTNA 4WJ, PBS, or Poly(I:C) as a positive control. The cells were then left for 18 h, and the amount of TNF- α was quantified using a human TNF- α ELISA kit. No innate immune response was observed for the aTNA 4WJ (Figure 3c).

Encouraged by the confirmation of the biocompatibility of the aTNA 4WJ, we next wanted to study the attachment of different moieties of interest to the 4WJ to alter its biodistribution and pharmacokinetics. We initially investigated the 4WJ for cancer cell targeting using a 4WJ nanobody conjugate in vitro. Nanobodies are single-domain camelid antibodies, that are generally very stable, and much smaller (around 16 kDa) than traditional antibodies.^[24] The chosen nanobody, 2Rb17c, binds human epidermal growth factor receptor 2 (HER2) with high specificity.^[25] The nanobody was specifically chosen as HER2 is a well-known breast cancer marker and biomolecular drugs, and imaging agents targeting this receptor have already been developed.^[26,27] For conjugation of an oligonucleotide to a protein of interest (POI) we have previously used DNA-templated protein conjugation, a method where a complementary DNA strand guides a DNA reacting strand into proximity of the POI.^[28] But as aTNA is more scarce than DNA, we wanted a method where only one equivalent of the aTNA strand of interest would need to be used to connect to the POI. Therefore, the nanobody 2Rb17c was expressed with an azido phenylalanine, using amber codon suppression for protein expression with unnatural amino acids.^[29] The unnatural amino acid was inserted at a position chosen from the crystal structure of 2Rb17c to have no interference with the binding domain.

An aTNA dibenzocyclooctyne (DBCO) oligo was prepared from aTNA-D, to react with the azido modified 2Rb17c in a strain-promoted 1,3-dipolar cycloaddition (SPAAC).^[30] The 2Rb17c-aTNA-D conjugate was prepared and mixed with the remaining strands for the 4WJ to study the formation of the Cy5-2Rb17c-4WJ. The mixture was left

for 30 min in PBS and analyzed by native gel electrophoresis (Figure S14). The Cy5-2Rb17c-4WJ forms with the same efficiency as the other prepared 4WJ constructs. Surprisingly, there is only negligible difference in the migration in the gel between the 4WJ with the nanobody attached and the naked 4WJ (Figure S6). Flow cytometry was then used to investigate the binding of the Cy5 and 2Rb17c modified

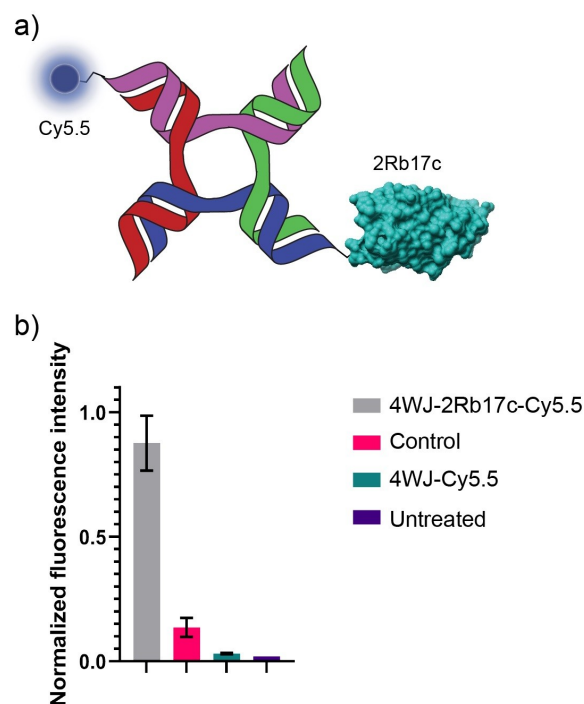


Figure 4. Investigation of the 2Rb17c-Cy5.5-4WJ construct. a) Illustration of the 2Rb17c-Cy5.5-4WJ construct. b) Flow cytometry data on SKBR3 (HER2+) using 2Rb17c-Cy5.5-4WJ or Cy5.5-4WJ. The control experiment is pretreatment of the cells with native 2Rb17c.

4WJ. The Cy5-2Rb17c-4WJ construct was therefore applied to SKBR3 (HER2+) cells, and the cells were further analyzed by flow cytometry (Figure 4b). A control experiment, where the HER2 receptors are saturated with unconjugated 2Rb17c before addition of the Cy5-2Rb17c-4WJ construct ensures that binding of the conjugated 2Rb17c remains to the original epitope of 2Rb17c. The construct effectively binds SKBR3 cells, and the binding can be diminished by pre-saturation of the epitope by 2Rb17c, which demonstrates that the 4WJ system is able to target cancer cells specifically *in vitro*. We envisage that the 4WJ can be used as a screening tool to investigate the combination effect of different cancer targeting moieties, without the use of elaborate chemistry for connection of the different targeting moieties.

Finally, an *in vivo* circulation study of the aTNA 4WJ was performed. Control of the serum half-life is important for biomolecular drugs and imaging agents alike. We expected that the relatively small diameter of the aTNA 4WJ, of approximately 17 nucleotides (5.6 nm), would give

rise to a low serum half-life *in vivo* due to glomerular filtration. We aimed to prolong this by functionalizing one and two of the aTNA arms with a palmitic acid (PA) modification, which is a modification known to extend the serum half-life by binding to endogenous serum albumin which has a circulatory half life of ≈ 19 days.^[31] Conjugates with PA modification(s) therefore remain for longer time in the bloodstream as they avoid glomerular filtration,^[32] as demonstrated in work by Jonassen and co-workers.^[33] The modification of biomolecules with PA, or other fatty acids can give rise to solubility issues.^[34] However, this was not thought to be the case for the 4WJ as aTNA is soluble in water to high millimolar concentrations because of the negatively charged phosphate backbone. Amino modified aTNA-A and aTNA-C were modified with a PA NHS ester, and a Cyanine 5.5 (Cy5.5) NHS ester was used to modify aTNA-B. Initially, we wanted to verify that the PA modified junction showed affinity towards albumin using a gel shift assay. For this the single PA modified junction, PA-Cy5.5-4WJ was used. Cy5.5-4WJ was also used as a control. Two

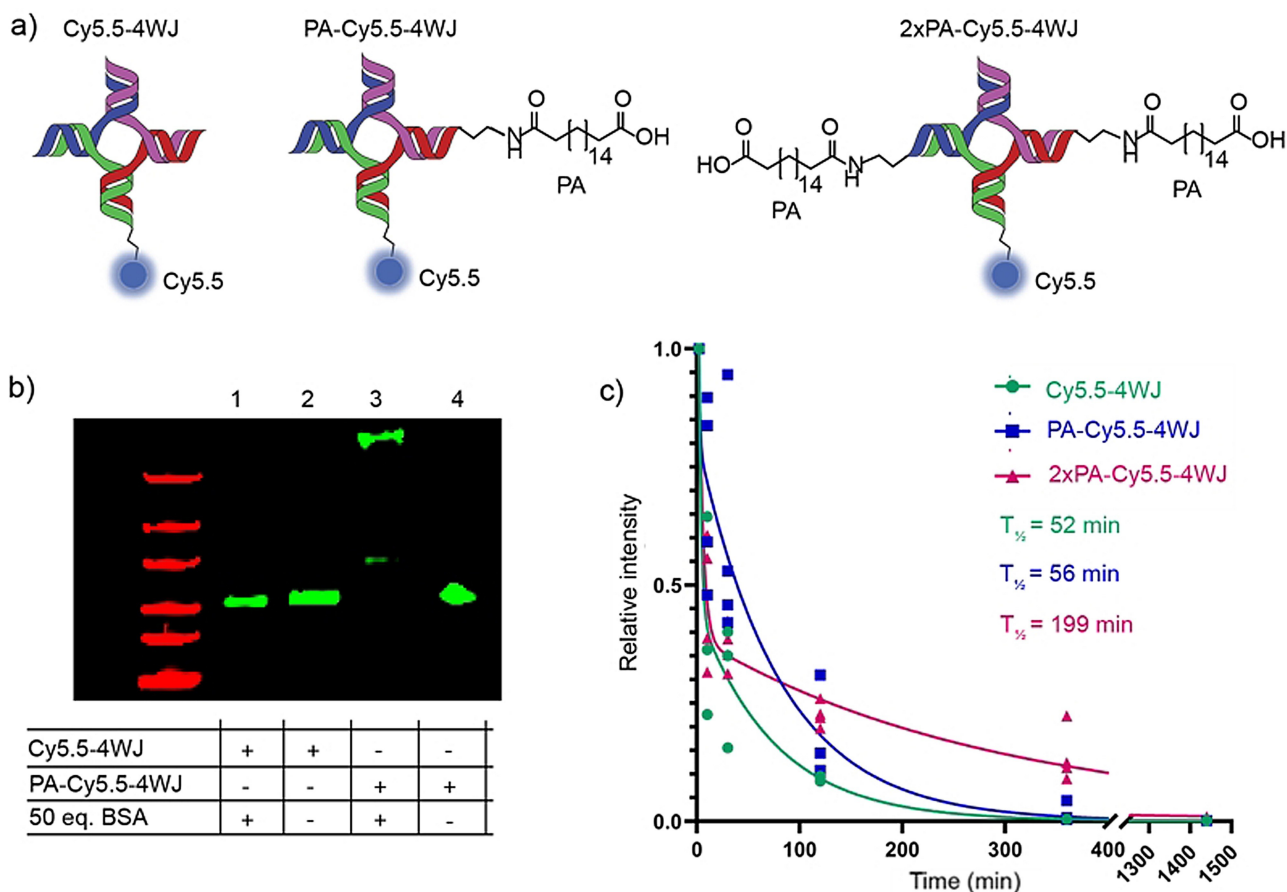


Figure 5. Investigation of the PA-Cy5.5-4WJ constructs. a) Illustration of the different 4WJ constructs used to investigate *in vivo* serum half-life. b) Gel shift assay of Cy5.5-4WJ and PA-Cy5.5-4WJ. Lane 1: Cy5.5-4WJ with 50 equiv BSA, Lane 2: Cy5.5-4WJ, Lane 3: PA-Cy5.5-4WJ + 50 equiv BSA, Lane 4: PA-Cy5.5-4WJ. Red is SybrGold scan, green is Cy5.5 scan. For full image see Figure S5 in the Supporting Information. c) Relative blood levels of 2xPA-Cy5.5-4WJ, PA-Cy5.5-4WJ and Cy5.5-4WJ in BALB/cAnNRj mice over 1440 min. A two-phase decay model was used to calculate the half-life of the three samples. Here half-life(slow) is reported, as this half-life is the actual, primarily renal, secretion of the sample from serum. The method is further explained in the Supporting Information.

samples of Cy5.5-4WJ and PA-Cy5.5-4WJ were prepared, to one of each was then given 50 equiv bovine serum albumin (BSA) and the samples were left for 2 h before being analyzed by native gel electrophoresis (Figure 5a). As seen in lane 3 the PA modified 4WJ binds to BSA which significantly lowers the mobility of the construct in the gel.

The serum half-life of the Cy5.5-4WJ was compared with PA-Cy5.5-4WJ and 2xPA-Cy5.5-4WJ in BALB/cAnNRj mice (Figure 5c). The clearance of the aTNA 4WJ follows a two-compartment pharmacokinetics model and a two-phase decay model was therefore used to calculate the half-life. This provides two half-life constants, half-life_{fast} and half-life_{slow}. Half-life_{fast} describes the initial uptake into organs, fatty tissue etc., where half-life_{slow} describes the actual clearance of the sample from blood, primarily through the kidney. Since this is the parameter, we are interested in altering, this is what we have reported here. Additional information on the method used can be found in the Supporting Information. The attachment of PA functionalities to the aTNA 4WJ does increase the serum half-life of the structure. Only a minor increase is observed with just one modification, but with two modifications the half-life of the structure is increased by almost a factor of four. It is also noticeable that after 24 h, only the construct with two PA modifications is still detectable in the serum.

In summary, we have shown the development and use of an aTNA 4WJ as a scaffold for in vivo applications. The junction consists of four 16 bases long aTNA strands that when mixed in equimolar amounts form the junction quantitatively. Each strand is furthermore modified with an amine, allowing for further functionalization of the 4WJ. Thermal denaturing showed that the junction melts at 69 °C in PBS buffer. We envisage the use of the 4WJ both as a drug delivery and research tool, and therefore investigated its compatibility with the attachment of different moieties and in vivo application. The junction showed no serum degradation in an overnight study, no non-targeted uptake, immunogenicity, or cytotoxicity. Furthermore, we have attached Cy5, Cy5.5, a DBCO, the nanobody 2Rb17c, and a palmitic acid modification to different oligos used in the 4WJ, all in good yield, and most importantly the 4WJ formed as expected with these modifications. A 4WJ construct with a nanobody and Cy5 was used for cancer cell targeting in vitro, and lastly, a PA and Cy5.5 modified 4WJ was used to prolong the serum half-life of the 4WJ in vivo. This last experiment shows that the pharmacokinetics and potentially biodistribution of the 4WJ can be predictably altered by modifying the 4WJ.

Acknowledgements

The work is funded by the Novo Nordisk foundation (CEMBID) (Grant Number NNF17OC0028070) and CellPAT (DNRF135).

Conflict of Interest

The authors declare no conflict of interest.

Data Availability Statement

The data that support the findings of this study are available on request from the corresponding author. The data are not publicly available due to privacy or ethical restrictions.

Keywords: DNA · Holliday Junction · Nanostructures · aTNA

- [1] N. R. Kallenbach, R.-I. Ma, N. C. Seeman, *Nature* **1983**, *305*, 829–831.
- [2] S. I. Liang, J. M. McFarland, D. Rabuka, Z. J. Gartner, *J. Am. Chem. Soc.* **2014**, *136*, 10850–10853.
- [3] L. Pan, C. Cao, C. Run, L. Zhou, J. J. Chou, *Adv. Sci.* **2020**, *7*, 1900973.
- [4] D. Jiang, Y. Sun, J. Li, Q. Li, M. Lv, B. Zhu, T. Tian, D. Cheng, J. Xia, L. Zhang, L. Wang, Q. Huang, J. Shi, C. Fan, *ACS Appl. Mater. Interfaces* **2016**, *8*, 4378–4384.
- [5] M. I. Setyawati, R. V. Kuttly, D. T. Leong, *Small* **2016**, *12*, 5601–5611.
- [6] Q. Zhang, Q. Jiang, N. Li, L. Dai, Q. Liu, L. Song, J. Wang, Y. Li, J. Tian, B. Ding, Y. Du, *ACS Nano* **2014**, *8*, 6633–6643.
- [7] T. Liu, P. Song, A. Märcher, J. Kjems, C. Yang, K. V. Gothelf, *ChemBioChem* **2019**, *20*, 1014–1018.
- [8] D. Jiang, C. G. England, W. Cai, *J. Controlled Release* **2016**, *239*, 27–38.
- [9] M. C. Chakrabarti, F. P. Schwarz, *Nucleic Acids Res.* **1999**, *27*, 4801–4806.
- [10] A. A. Koshkin, P. Nielsen, M. Meldgaard, V. K. Rajwanshi, S. K. Singh, J. Wengel, *J. Am. Chem. Soc.* **1998**, *120*, 13252–13253.
- [11] R. S. Zhang, E. O. McCullum, J. C. Chaput, *J. Am. Chem. Soc.* **2008**, *130*, 5846–5847.
- [12] S. A. Kazane, J. Y. Axup, C. H. Kim, M. Ciobanu, E. D. Wold, S. Barluenga, B. A. Hutchins, P. G. Schultz, N. Winssinger, V. V. Smider, *J. Am. Chem. Soc.* **2013**, *135*, 340–346.
- [13] V. L. Andersen, M. Vinther, R. Kumar, A. Ries, J. Wengel, J. S. Nielsen, J. Kjems, *Theranostics* **2019**, *9*, 2662–2677.
- [14] R. D. Youssefeyeh, J. P. H. Verheyden, J. G. Moffatt, *J. Org. Chem.* **1979**, *44*, 1301–1309.
- [15] S. K. Singh, P. Nielsen, A. A. Koshkin, J. Wengel, *Chem. Commun.* **1998**, 455–456.
- [16] S. Siddiquee K Rovina, A. Azriah, *Adv. Tech. Biol. Med.* **2015**, *3*, 1000131.
- [17] K. Murayama, H. Kashida, H. Asanuma, *Chem. Commun.* **2015**, *51*, 6500–6503.
- [18] H. Asanuma, T. Toda, K. Murayama, X. Liang, H. Kashida, *J. Am. Chem. Soc.* **2010**, *132*, 14702–14703.
- [19] V. Kumar, V. Kesavan, K. V. Gothelf, *Org. Biomol. Chem.* **2015**, *13*, 2366–2374.
- [20] V. Kumar, K. V. Gothelf, *Org. Biomol. Chem.* **2016**, *14*, 1540–1544.
- [21] T. J. D. Nguyen, I. Manuguerra, V. Kumar, K. V. Gothelf, *Chem. Eur. J.* **2019**, *25*, 12303–12307.
- [22] V. Kumar, T. J. D. Nguyen, J. Palmfeldt, K. V. Gothelf, *Org. Biomol. Chem.* **2019**, *17*, 7655–7659.
- [23] H. J. Park, Y. Zhang, J. Naggar, S. P. Georgescu, D. Kong, J. B. Galper, *Perinat. Stem Cells* **2010**, *5*, 169–188.
- [24] I. Van Audenhove, J. Gettemans, *e-biomed* **2016**, *8*, 40–48.

- [25] I. Vaneycken, N. Devoogdt, N. Van Gassen, C. Vincke, C. Xavier, U. Wernery, S. Muyltermans, T. Lahoutte, V. Cavaliere, *FASEB J.* **2011**, *25*, 2433–2446.
- [26] A. V. F. Massicano, B. V. Marquez-Nostra, S. E. Lapi, *Mol. Imaging* **2018**, *17*, 1536012117745386.
- [27] G. Rinnerthaler, S. P. Gampenrieder, R. Greil, *Int. J. Mol. Sci.* **2019**, *20*, 1115.
- [28] C. B. Rosen, A. L. B. Kodal, J. S. Nielsen, D. H. Schaffert, C. Scavenius, A. H. Okholm, N. V. Voigt, J. J. Enghild, J. Kjems, T. Tørring, K. V. Gothelf, *Nat. Chem.* **2014**, *6*, 804–809.
- [29] H. Xiao, A. Chatterjee, S. H. Choi, K. M. Bajjuri, S. C. Sinha, P. G. Schultz, *Angew. Chem. Int. Ed.* **2013**, *52*, 14080–14083; *Angew. Chem.* **2013**, *125*, 14330–14333.
- [30] X. Ning, J. Guo, M. A. Wolfert, G. J. Boons, *Angew. Chem. Int. Ed.* **2008**, *47*, 2253–2255; *Angew. Chem.* **2008**, *120*, 2285–2287.
- [31] E. G. W. Schmidt, M. L. Hvam, F. Antunes, J. Cameron, D. Viuff, B. Andersen, N. N. Kristensen, K. A. Howard, *J. Biol. Chem.* **2017**, *292*, 13312–13322.
- [32] A. Zorzi, S. J. Middendorp, J. Wilbs, K. Deyle, C. Heinis, *Nat. Commun.* **2017**, *8*, 16092.
- [33] I. Jonassen, S. Havelund, T. Hoeg-Jensen, D. B. Steensgaard, P. O. Wahlund, U. Ribel, *Pharm. Res.* **2012**, *29*, 2104–2114.
- [34] M. F. T. Koehler, K. Zobel, M. H. Beresini, L. D. Caris, D. Combs, B. D. Paasch, R. A. Lazarus, *Bioorg. Med. Chem. Lett.* **2002**, *12*, 2883–2886.

Manuscript received: November 10, 2021

Accepted manuscript online: March 30, 2022

Version of record online: April 13, 2022